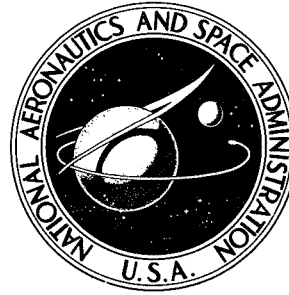


N70-34796

NASA TECHNICAL NOTE



NASA TN D-5927

NASA TN D-5927

p - p AND p - t FINAL
STATE INTERACTIONS IN
THE REACTION ${}^3\text{He}(d, tp)p$

by

*R. E. Warner, B. E. Corey, and E. L. Petersen
Oberlin College*

*R. W. Bercau
Lewis Research Center*

and

*J. E. Poth
Miami University*

CASE FILE
COPY

1. Report No. NASA TN D-5927	2. Government Accession No.	3. Recipient's Catalog No.	
4. Title and Subtitle p - p AND p - t FINAL STATE INTERACTIONS IN THE REACTION ${}^3\text{He}(d, tp)p$		5. Report Date August 1970	6. Performing Organization Code
		8. Performing Organization Report No. E-5383	
7. Author(s) R. E. Warner, B. E. Corey, E. L. Petersen, R. W. Bercaw, and J. E. Poth (see following page for affiliation)		10. Work Unit No. 129-02	11. Contract or Grant No.
9. Performing Organization Name and Address Lewis Research Center National Aeronautics and Space Administration Cleveland, Ohio 44135		13. Type of Report and Period Covered Technical Note	
		14. Sponsoring Agency Code	
12. Sponsoring Agency Name and Address National Aeronautics and Space Administration Washington, D. C. 25046		15. Supplementary Notes	
16. Abstract Absolute coincidence cross sections were measured for the reaction ${}^3\text{He}(d, tp)p$ at $E_d = 20.7$ MeV. Deep minima were observed in the cross sections when the relative energy of either $p + p$ or $t + p$ was below ~ 20 keV. Predictions of the Watson-Migdal theory and of the PWBA and DWBA theories of Henley, Richards, and Yu gave good agreement with the shapes of the spectra near these minima, but the required normalization factors varied widely from one geometry to another. Decay of the 21.2-MeV ${}^4\text{He}$ state, but not the 20.0-MeV state, was observed.			
17. Key Words (Suggested by Author(s))		18. Distribution Statement Unclassified - unlimited	
19. Security Classif. (of this report) Unclassified	20. Security Classif. (of this page) Unclassified	21. No. of Pages 25	22. Price* \$3.00

Authors: R. E. Warner, B. E. Corey, and E. L. Petersen, Oberlin College, Oberlin, Ohio; R. W. Bercaw, Lewis Research Center; and J. E. Poth, Miami University, Oxford, Ohio

p - p AND p - t FINAL STATE INTERACTIONS IN THE REACTION ${}^3\text{He}(d, tp)p$

by R. E. Warner,* B. E. Corey,* E. L. Petersen,*
R. W. Bercaw, and J. E. Poth†

Lewis Research Center

SUMMARY

Absolute coincidence cross sections were measured for the reaction ${}^3\text{He}(d, tp)p$ at $E_d = 20.7$ MeV. Deep minima were observed in the cross sections when the relative energy of either $p + p$ or $t + p$ was below ~ 20 keV. Predictions of the Watson-Migdal theory and of the PWBA and DWBA theories of Henley, Richards, and Yu gave good agreement with the shapes of the spectra near these minima, but the required normalization factors varied widely from one geometry to another. Decay of the 21.2-MeV ${}^4\text{He}$ state, but not the 20.0-MeV state, was observed.

INTRODUCTION

There have been two coincidence studies of the nuclear reaction ${}^3\text{He} + d \rightarrow t + 2p$. Parker et al. (ref. 1) used 32-MeV incident ${}^3\text{He}$ ions, and observed prominent triton-proton final-state interactions (FSI) resulting from the decay of two states at 19.94- and 21.24-MeV excitation in ${}^4\text{He}$; Zurmuhle (ref. 2), using an 18-MeV ${}^3\text{He}$ beam observed only the 21.2-MeV ${}^4\text{He}$ state. Both groups concluded that the $p - p$ FSI was unimportant. In contrast, several experimental groups (refs. 3 to 6) have observed noncoincident tritons from this reaction and concluded that the high-energy triton spectra were dominated by the $p - p$ FSI.

A recent article by Henley, Richards, and Yu (ref. 7) (hereinafter called HRY) contains the most complete theoretical study of this reaction to date. They explicitly take into account the $p - p$ FSI by computing exact scattering wave functions for the two

*Oberlin College, Oberlin, Ohio; research supported by the National Science Foundation.

†Miami University, Oxford, Ohio; NASA-ASEE Faculty Fellow, 1968.

product protons, assuming that they interact through a point Coulomb plus a Woods-Saxon real central nuclear potential. Gaussian internal wave functions were used for the deuteron, triton, and ^3He ; and wave functions for the relative motions of the two- and three-nucleon groups were computed in both plane-wave (PWBA) and distorted-wave (DWBA) Born approximations. The contributions of both pickup and charge exchange processes to the transition matrix element were included, but the effects of the ^4He excited states were neglected.

The present coincidence study has two objectives: (1) to try to determine which FSI are important, and (2) to test the ability of HRY's PWBA and DWBA theories to predict absolute coincidence cross sections. They have previously been used to analyze only noncoincidence experiments (refs. 4 and 5). Comparisons with the predictions of the Watson-Migdal theory, which treats FSI to first order but fails to provide an absolute normalization, also are made.

EXPERIMENTAL PROCEDURE AND RESULTS

Most experimental details were similar to those in an earlier study (ref. 8) of the $D(\alpha, \alpha p)n$ reaction. The 20.7-MeV deuteron beam of the NASA-Lewis Cyclotron was analysed and focused on a 10-centimeter-diameter cell containing ^3He gas at the center of a 150-centimeter-diameter scattering chamber. A Faraday cup measured the total charge, and measurements of the gas cell temperature and pressure (45 to 190 torr) determined the target density to within 3 percent.

Tritons were detected by a two-counter telescope with a 6-MeV threshold, and protons by a single counter; these two detectors were coplanar with, and on opposite sides of, the beam. The triton telescope subtended 0.98 milliradian in the first of two experimental runs and 0.61 milliradian in the second. Its mount also held a slit adjacent to the target cell which defined the effective target volume. The proton counter subtended 0.86 milliradian in both runs. Fast-slow coincidences allowed the triton signals to be presented to a power-law particle identifier (ref. 9). This device gated a two-dimensional pulse height analyzer, which stored coincident triton and proton signals. The mass resolution was nearly perfect, but at two geometries $[(\theta_t, \theta_p)$ equal to $(25^\circ, 40^\circ)$ and $(25^\circ, 55^\circ)$] the identifier accepted a few deuterons, allowing events from the $d + ^3\text{He} \rightarrow d + d + p$ reaction to be recorded. These were easily rejected by kinematical considerations since the sum of the detected particle energies was at least 2.5 MeV less than in the reaction being studied.

Random coincidence rates were measured in separate runs with the proton signal delayed by two cyclotron radiofrequency cycles. They were normalized by comparing the delayed and nondelayed rates in portions of the spectra for which no real coinci-

dences are possible. This normalization method eliminated possible errors resulting from (1) different beam intensities in nondelayed and delayed runs, (2) microstructure in the beam causing successive beam bursts to have different intensities, and (3) the added delay not being exactly two radiofrequency periods. The data were analyzed by a computer program which located events kinematically attributable to this reaction, subtracted random coincidence background, and computed absolute cross sections and their statistical uncertainties. All reported uncertainties are statistical only; additional systematic errors are believed to be less than 10 percent.

Our data for 12 geometries and the results of our calculations (see next section) are shown in figure 1. The cross sections are plotted against the proton laboratory kinetic energy E_p , and the kinetic energy of the two protons in their own center-of-mass system ϵ_{pp} . For certain geometries, the parameter ϵ_{pp} , the more significant one for the p - p FSI, attains very small minimum values. When (θ_t, θ_p) equals $(50^\circ, 45^\circ)$, $(25^\circ, 80^\circ)$, and $(35^\circ, 70^\circ)$, these minimum values are 0.001, 0.01, and 0.02 MeV, respectively. Deep minima of the cross sections are observed at these minima of ϵ_{pp} ; this effect, the result of Coulomb repulsion in the final state, was also observed in the reactions ${}^3\text{He}({}^3\text{He}, p\alpha)p$ (ref. 10) and ${}^3\text{He}(p, pd)p$ (ref. 11). Chang et al. (ref. 11) found that the ${}^3\text{He}(p, pd)p$ cross sections reached maxima for $\epsilon_{pp} \approx 0.5$ MeV and gradually decreased for larger ϵ_{pp} . Our data do not clearly show this effect, but often such a decrease could be masked by the ${}^4\text{He}$ excited state at 21.2 MeV.

The arrows labeled He in figure 1 mark the locations where the relative kinetic energy of triton and undetected proton equals 21.2 MeV minus the ${}^4\text{He} \rightarrow t + p$ dissociation energy (19.812 MeV). Large peaks are, in fact, observed at or near all but one $(35^\circ, 70^\circ)$ of the nine kinematically possible locations, and the existence of the previously reported (refs. 1 and 2) 21.2-MeV level in ${}^4\text{He}$ is thus confirmed.

Any group from the 19.94-MeV level reported by Parker et al. (ref. 1) would come near the maximum laboratory proton energies observed in this experiment, where the cross section projected on the E_p axis is dominated by kinematic singularities. The cross sections are therefore projected upon the triton energy axis (in fig. 2) for the four geometries where the t + p relative energy becomes small enough for the level to be observed. The arrows labelled 19.94 and 21.2 in figure 2 show the expected locations of groups from the 19.94- and 21.2-MeV levels, respectively. Peaks from the higher level are always observed but often distorted in shape by the increased phase space caused by the near-maximum triton energy. Since the reported width of the 19.94-MeV level is $\Gamma = 0.14$ MeV, a group from this state should enhance the cross section at all t - p relative energies below 0.2 MeV. Thus the two elevated data points near $E_t = 7$ MeV at $(25^\circ, 70^\circ)$ can be assumed to be statistical fluctuations, and we conclude that the 19.94-MeV level is not populated in this experiment. An interesting effect is seen in the two lower parts of figure 2; pronounced minima in the cross section coincide with the deep minima (0.01 MeV) in the t - p relative energy. The explanation

is presumably the same as the for minima due to the p - p interaction: the strong repulsive Coulomb interaction between t and p in the final state reduces the reaction probability.

THEORY AND ANALYSIS

In this section, we discuss the results of three theories used to predict cross sections for this reaction: the PWBA and DWBA formulations of Henley, Richards, and Yu (ref. 7), and the Watson-Migdal theory (refs. 5, 12, and 13).

PWBA Analysis

A brief summary of the equations obtained by HRY follows. The potential through which two nucleons interact during the reaction is taken to be

$$V(r) = -\frac{1}{2} V_c (1 - BP_\tau P_\sigma) \exp(-\beta^2 r^2) \quad (1)$$

where P_τ and P_σ are isospin- and spin-exchange operators, $V_c = 207$ MeV, $\beta = 0.632$ femtometer⁻¹, and $B = 1.5$. The squared matrix element, averaged over initial spin states and summed over final states, is

$$\bar{\sum}_{if} |M|^2 = \frac{\left| (1+B) TI_{PU} - \frac{1}{2} B SI_{CE} \right|^2}{18} \quad (2)$$

where TI_{PU} and SI_{CE} are the amplitudes for pickup and charge-exchange. These are obtained from the equations

$$I_{PU} = \text{Constant} \times \int_0^\infty U_q^{(-)*}(r) e^{-3\gamma^2 r^2/4} r dr \quad (3)$$

$$I_{CE} = \text{Constant} \times \int_0^\infty U_q^{(-)*}(r) j_0\left(\frac{1}{2} Pr\right) U_d(r) dr \quad (4)$$

$$T = \text{Constant} \times \int_{r_c}^{\infty} e^{-\gamma^2 z^2} \sin(Qz) z dz \int_0^{\infty} \sin(Q'y) e^{-y^2(\gamma^2 + \beta^2)} dy$$

$$\times \int_0^{\infty} U_d(r) e^{-r^2(1.5 \gamma^2 + 0.25 \beta^2)} (e^{\beta^2 r y} - e^{-\beta^2 r y}) r dr \quad (5)$$

$$S = \text{Constant} \times \int_{r_c}^{\infty} e^{-\beta^2 y^2} \sin(Py) y dy \int_0^{\infty} e^{-\gamma^2 z^2} \left(\sin \frac{2}{3} Pz \right) z dz \quad (6)$$

$$\left. \begin{aligned} \bar{Q} &= \frac{2}{3} \bar{K} - \bar{k} \\ \bar{Q}' &= \bar{K} - \frac{2}{3} \bar{k} \\ \bar{P} &= \bar{K} + \bar{k} \end{aligned} \right\} \quad (7)$$

In these formulas, the integrations over the angular parts of the wave functions have been carried out. The relative momentum of the two protons in their center-of-mass system is $\hbar \bar{q}$, and the momenta of the incident deuteron and the final triton in the overall center-of-mass system are $\hbar \bar{K}$ and $\hbar \bar{k}$, respectively. Equation (3) contains the effect of the FSI of the two protons on the pickup process; $U_q^{(-)*}$ describes their relative motion in the final state, while $\exp(-3\gamma^2 r^2/4)$ gives their spatial dependence in the original ${}^3\text{He}$ nucleus. An analysis (ref. 14) of electron scattering data yields $\gamma = 0.36$ femtometer $^{-1}$. Similarly, equation (4) describes the effect of the p - p interaction on the charge-exchange process. Here the two protons which interact in the final state were originally the two nucleons in the deuteron, whose wave function is U_d . The PWBA curves in figure 1 were computed using Gaussian deuteron-wave functions

$$U_d(r) = N \exp\left(-\frac{1}{2} a^2 r^2\right) \quad (8)$$

and zero cutoff radii r_c . The p - p wave function $U_q^{(-)*}(r)$ was computed by assuming a

point Coulomb interaction and a Woods-Saxon central nuclear potential

$$V(r) = -V_0 \left[1 + \exp\left(\frac{r - R_0}{a}\right) \right]^{-1} \quad (9)$$

with parameters ($V_0 = 33.5$ MeV, $R_0 = 1.477$ fm, $a = 0.5$ fm) which reproduced the accepted values (ref. 15) of the p - p scattering length a_{pp} (-7.7 fm) and effective range r_{eff} (2.7 fm).

Several parameters were varied individually in an effort to improve the PWBA fits and minimize the variation of the normalizing factors (indicated in fig. 1) from one geometry to another. Figure 3 shows the effect of varying the force parameter B (eq. (1)) and the cutoff radius r_c (eqs. (5) and (6)) at ($35^\circ, 70^\circ$). Equation (2) shows that the pickup and charge-exchange amplitudes are proportional to $1 + B$ and B , respectively. The computed cross sections in figure 3(a) are divided by $(1 + B)^2$. Thus the three curves would coincide if the reaction mechanism were pure pickup. For $\theta_t \geq 30^\circ$ the pickup to charge-exchange amplitude ratio was typically 2:1; for smaller θ_t it was usually much larger. Therefore, no value of B exists which will eliminate the large variation in normalizing factors.

An intuitive picture of the reaction suggests that high-energy tritons emitted near 0° in the overall center-of-mass system should come mainly from the pickup process, while those emitted near 180° should result from charge-exchange. Near 0° , the kinematic quantities in equation (7) have the values $P \approx 2K$ and $Q \approx K/3 \approx Q'$ for the highest energy tritons emitted (neglecting the reaction Q -value), while $P \approx 0$ and $Q \approx 5K/3 \approx Q'$ near 180° . Thus, in the theory, the charge-exchange amplitude is small near 0° because the large P causes rapid oscillations in the integrands of both equations (4) and (6). Similarly, near 180° , I_{CE} is large since $j_0(Pr/2) \rightarrow 1$, and T is small due to rapid oscillation of the functions $\sin(Qz)$ and $\sin(Q'z)$ in equation (5).

Figure 3(b) shows that the cross section decreases with increasing cutoff radius. With the large values of r_c used by HRY (5.8 and 6.8 fm for charge-exchange and pickup amplitudes, respectively), only the extreme tails of the triton wave function (for pickup) and the nuclear force (for charge-exchange) contribute to the matrix element, and our predictions would have been about 10^5 times too small. The rationale for introducing cutoffs is to allow for absorption of the incident wave; their principal effect here, apart from normalization, is to change the ratio of charge-exchange to pickup in a rather arbitrary way. We used $r_c = 0$, having concluded that no general improvement in the fits could be obtained by using any other value.

Figure 4 shows the effect of varying the parameters of the p - p nuclear potential. We obtained $a_{pp} = -7.7$ femtometers and $r_{\text{eff}} = 3.3$ femtometers with $V_0 = 16.0$ MeV, $R_0 = 2.247$ femtometers, and $a = 0.5$ femtometer; while $a_{pp} = -4.4$ femtometers

and $r_{\text{eff}} = 2.7$ femtometers were obtained with $V_0 = 50.0$ MeV, $R_0 = 1.006$ femtometers, and $a = 0.5$ femtometers. The three curves give about equally good fits to the data and it is clear that experiments of this type cannot give new information about the $p - p$ scattering length and effective range, particularly since the theory gives incorrect normalization.

Finally, four different deuteron-wave functions were tried: the Gaussian (eq. (8)), the Hulthen (eq. (4) of ref. 7), the wave function for a square well which reproduces the $n - p$ triplet scattering length and effective range (ref. 16), and the Moravcsik "Approximation III" wave function (ref. 17). At $(35^\circ, 70^\circ)$ the Moravcsik predictions were about 10 percent lower than the average for the first three, which agreed to about ± 3 percent.

DWBA Analysis

The necessary formulas for this analysis are given by HRY (ref. 7) and will not be repeated here. This work differs from that of the last section in that the wave functions for relative motion of the ${}^3\text{He}$ and deuteron in the initial state, and for the triton and diproton in the final state, are found by solving the wave equation numerically, assuming a complex central interaction. In their optical model analysis of elastic deuteron scattering from medium- A nuclei, Perey and Perey (ref. 18) found it preferable to use surface absorption in which the imaginary potential shape is taken to be the derivative of equation (8). For mass $A = 3$ the distinction between surface and volume effects seems irrelevant, and we used the Woods-Saxon shape (eq. (8)) for both real and imaginary parts of the optical potential. Partial waves up to $l = 7$ were included, and matrix element inaccuracies due to dropping higher partial waves were less than 0.1 percent. Although contributions of the $l \geq 4$ waves to the matrix elements were generally small because of the centrifugal barrier, the $l = 3$ wave often gave the largest contribution since the $l \leq 2$ waves oscillated inside the nuclear potential causing cancellation in the integrals in equations (32a) and (34b) of HRY (ref. 7).

Figure 5 shows the results obtained at $(35^\circ, 70^\circ)$ with several sets of optical model parameters, which are listed in table I. A triton charge radius (ref. 19) of 1.25 femtometers $\times A^{1/3}$ was used, and the diffuseness a was 0.6 femtometer in all cases; note that $r_0 A^{1/3}$ equals the R_0 of equation (8).

Several workers (refs. 18, and 20 to 22, and E. Vogt in a private communication) have proposed that the optical potentials for bombarding particles of mass A should be A times the nucleon potentials. For instance, among the potentials investigated by Perey and Perey (ref. 18), the one (type b) which was the closer approximation to a sum χ^2 in fitting a large selection of deuteron elastic scattering data. The accepted values (ref. 15 and E. Vogt) for the nucleon optical potential strength $V_0 r_0^2$ are about 80 MeV-femtometers squared. Therefore, we used parameter set 1 (table I), for which

$V_0 r_0^2 = 160$, for the calculations shown in figure 1. This set represents a slight modification of the potential used by Melkanoff et al. (ref. 23) for deuteron elastic scattering from complex nuclei at 11.8 MeV, which is close to the center-of-mass bombarding energy (12.5 MeV) of this experiment. Sets 2, 3, and 4 are potentials which have been used for deuteron scattering from light nuclei; for all of these, $V_0 r_0^2$ ranges from 108 to 192 MeV-femtometers squared. Set 5, originally used by HRY, has $V_0 r_0^2 = 840$ MeV-femtometers squared which is five times larger than the accepted value.

It would have been of interest to find a parameter set which required equal normalization factors at all geometries since (assuming the reaction proceeds by pickup) a spectroscopic factor for decomposition of ${}^3\text{He}$ into a neutron plus diproton could then have been deduced. Figure 1 shows that the normalization factors required for set 1 vary by a factor of 20, and even larger variations were found for the other sets. Also, no improvement was obtained by small variations from set 1; therefore, we have been unable to obtain a fully satisfactory set of optical model parameters. It has already been observed (ref. 7) that the optical model may not be applicable to such light nuclei.

With $B = 1.0$, the pickup to charge-exchange amplitude ratio was nearly always at least 10:1. Therefore, it was even less feasible to improve the quality of fits by varying this parameter than it was in the PWBA studies.

Watson-Migdal Analysis

In this analysis (refs. 3, 5, 6, 12, and 13) the FSI between protons (assumed to be in an s -state) is taken into account, while the rest of the interaction is simply assumed to multiply the matrix element by a constant. The matrix element was computed from equation (6) of reference 5. Several Watson-Migdal curves having arbitrary normalization are shown in figure 1. The fits obtained are generally as good as the PWBA and DWBA fits. This was equally true at other geometries, where Watson-Migdal curves were omitted to avoid crowding. Tombrello and Bacher (ref. 24) also have obtained good Watson-Migdal fits to the high-energy triton spectra obtained in a noncoincidence study of this reaction. Good Watson-Migdal fits also were obtained in the two cases where deep minima in the cross section resulted from relative t - p energies of about 10 keV; these are shown in the two lower parts of figure 2. The formulas used were

$$\frac{d^3\sigma}{d\Omega_p d\Omega_t dE_t} \propto c^2 \rho(E) \left\{ \frac{1}{4} \left[k^2 c^4 + \left(\frac{1}{2} r_1 k^2 - \frac{1}{a_1} - \frac{H(\eta)}{R} \right)^2 \right]^{-1} + \frac{3}{4} \left[k^2 c^4 + \left(\frac{1}{2} r_3 k^2 - \frac{1}{a_3} - \frac{H(\eta)}{R} \right)^2 \right]^{-1} \right\} \quad (10)$$

$$k^2 = \frac{2\mu\epsilon}{\hbar^2} \quad (11)$$

$$R = \frac{\hbar}{2\mu e^2} = 14.41 \text{ fm} \times \left(\frac{m_p}{\mu}\right) \quad (12)$$

$$\eta = \frac{e^2}{\hbar v} \quad (13)$$

where $\rho(E)$ is the density of final states and m_p is the proton mass. The relative energy, relative velocity, and reduced mass in the $t - p$ system are ϵ , v , and μ . The Coulomb penetration factor $C(\eta)$ and the function $H(\eta)$ are defined in reference 5. The $t - p$ scattering lengths in the 1S and 3S states are a_1 and a_3 , and the corresponding effective ranges are r_1 and r_3 . The calculations shown in figure 2 were done with $a_1 = -10$ femtometers, $a_3 = 5$ femtometers, $r_1 = 3$ femtometers, and $r_2 = 5$ femtometers; these parameters reproduce the Frank-Gammel (ref. 25) $t - p$ phase shifts for $\epsilon \leq 1$ MeV. The fits obtained are not quite as good as for the $p - p$ FSI. Nevertheless, the predicted minima for low relative energies are observed in both the $p - p$ and $t - p$ cases.

DISCUSSION

In figure 1 it is seen that, whenever $\epsilon_{pp} \leq 1$ MeV, the shapes of the PWBA and DWBA curves are nearly identical, except in one case ($50^\circ, 45^\circ$) where the difference results from substantial interference between pickup and charge-exchange amplitudes in the PWBA matrix element. For the other cases, the charge-exchange amplitude nearly vanishes and the triton energy E_t varies quite slowly with E_p . Since E_t and θ_t determine the factor T of the pickup amplitude, the PWBA matrix element is essentially a constant times I_{PU} . The functional form of the quantity corresponding to T is different in the DWBA treatment, but again it is nearly independent of E_p , and for the same reasons. Consequently, both matrix elements are proportional to the common factor $I_{PU}(\epsilon_{pp})$ which describes the $p - p$ interaction.

Haybron (ref. 26) has rigorously discussed the conditions under which the PWBA and Watson-Migdal theories give identical predictions. One requirement is that terms of order $r_{\text{eff}} R_0 k^2$ must be ignorable, where R_0 is the $p - p$ nuclear force range and $\hbar^2 k^2 = 2\mu\epsilon_{pp}$. In addition, one of the two following statements must be true: either (1) the pickup process predominates over charge-exchange and the function $\exp(-3\gamma^2 r^2/4)$

in our equation (3) falls off rapidly enough with increasing r to cut off terms of order $r_{\text{eff}}^2 k^2$, or (2) charge-change predominates over pickup and $U_d(r)$ in equation (4) falls off rapidly. The second requirement is a quantitative state of Watson's (ref. 12) original principle that the two particles which interact in the final state must initially be located in a small volume. Thus Haybron concludes that for this reaction the W-M theory is marginally applicable for pickup, where the two protons come from the initial ${}^3\text{He}$, but not for charge-exchange, where they come from the deuteron. Since our data are generally for the pickup region, this accounts for the general agreement between all three theories for small ϵ_{pp} , as shown in our figure 1. Haybron noted that his conclusions might be altered by the inclusion of distorted-wave effects; it is therefore very interesting that, at $(50^\circ, 45^\circ)$ where there is strong interference between pickup and charge-exchange, the DWBA and W-M curves are identical but differ substantially from the PWBA curve.

In figure 6, proton angular distributions are presented for three values of ϵ_{pp} at fixed $\theta_t = 25^\circ$. These are plotted against θ_{pp} , the angle of emission of the detected proton in the p - p center-of-mass system. Within the limited statistical accuracy, the cross section divided by phase space is isotropic with respect to θ_{pp} . Such isotropy also is predicted by the PWBA equations (2) to (6). This provides further evidence that an s-state p - p interaction has been observed.

A state in ${}^4\text{He}$ near 20.0 MeV with a width $\Gamma \approx 0.2$ MeV has been observed in the reactions ${}^3\text{He}(d, tp)p$ (ref. 1), $T(d, n){}^4\text{He}^*$ (refs. 27 and 28), ${}^1\text{H}(t, t){}^1\text{H}$ (refs. 29 and 30), ${}^6\text{Li}(p, {}^3\text{He}){}^4\text{He}^*$ (ref. 31), and ${}^7\text{Li}(p, \alpha){}^4\text{He}^*$ (ref. 31). Our failure to observe it in this experiment may therefore be attributable to the reaction mechanism. If the triton is first formed and then interacts with one of the protons for a time $\tau \sim \hbar/\Gamma \sim 3 \times 10^{-21}$ second, the probability of interacting with just one proton may be greater if the two protons originate in the loosely bound deuteron (charge-exchange process) rather than the tightly bound ${}^3\text{He}$ (pickup process). As was previously explained, our own data were taken in the pickup region; in contrast, Parker et al. (ref. 1) studied the same reaction using incident ${}^3\text{He}$ nuclei and detecting tritons, so their observations probably were mainly in the charge-exchange region.

CONCLUSIONS

Absolute coincidence cross sections were measured for the reaction ${}^3\text{He}(d, tp)p$ at $E_d = 20.7$ MeV. In conclusion, we find that

1. The minimum in the cross section for very low relative energy is a general feature of the interaction of two charged particles, having been observed for both the p - p and t - p systems and predicted by theory.

2. All three theoretical treatments (PWBA, DWBA, and Watson-Migdal) used in this analysis give fairly good fits to the observed spectra near the p - p minima. However, the required normalization factors for PWBA and DWBA vary widely from one geometry to another; no variations in the DWBA force constants or other parameters will overcome this problem.

3. The 21.2-MeV state of ${}^4\text{He}$ has been observed. The 19.94-MeV state has not, possibly for reasons related to the reaction mechanism.

It is a special pleasure for one of us (R. E. W.) to thank Professor Erich Vogt and Professor Ernest Henley for stimulating discussions which enhanced his understanding of the theory of this reaction. Glenn Flierl, Jeffrey Daines, Douglas Brown, and the staff of the Oberlin College Computer Center gave us valuable computational assistance.

Lewis Research Center,
National Aeronautics and Space Administration,
Cleveland, Ohio, January 20, 1970,
129-02.

APPENDIX - SYMBOLS

A	nuclear mass number	Q, Q'	linear combination of \vec{K} and \vec{k}
a	diffuseness	R_0	charge radius
a_{pp}	scattering length	r	radius
B	force parameter	r_c	cutoff radius
$C(\eta)$	Coulomb penetration factor	r_{eff}	effective range
c	velocity of light	r_0	charge radius divided by $A^{1/3}$
E_d	deuteron energy	S	integral in charge-exchange amplitude
E_p	proton energy	SI_{CE}	amplitude for charge exchange
E_t	triton energy	T	integral in pickup amplitude
\hbar	Plack constant/ 2π	TI_{PU}	amplitude for pickup
$\vec{\hbar K}$	momentum of incident deuteron	U_d	wave function for deuteron
$\vec{\hbar k}$	momentum of final triton	$U_q^{(-)*}$	wave function for relative motion of two protons in the final state
$\vec{\hbar q}$	relative momentum of two protons in their center-of-mass system	V_C	potential parameter
I_{CE}	integral in charge-exchange amplitude	V_0	potential parameter
I_{PU}	integral in pickup amplitude	v	relative velocity in the t - p center of mass system
j_0	zeroth-order spherical Bessel function	W_0	imaginary part of nuclear potential well
\vec{K}	wave number of incident deuteron	y, z	integration variable
\vec{k}	wave number of final triton	β	range parameter for nucleon-nucleon potential
l	angular momentum quantum number	γ	triton wave function parameter
m_p	proton mass	ϵ	energy in the t - p center-of-mass system
P	linear combination of \vec{K} and \vec{k}	ϵ_{pp}	relative energy of two protons in p - p center-of-mass system
P_τ	isospin-exchange operator		
P_σ	spin-exchange operator		

θ_{pp}	proton scattering angle in p - p center-of-mass system	ρ	phase space factor
θ_t	triton scattering angle (laboratory)	σ	cross section
θ_p	proton scattering angle (laboratory)	Ω_p	proton solid angle
μ	reduced mass in the t - p center of mass system	Ω_t	triton solid angle

REFERENCES

1. Parker, P. D.; Donovan, P. F.; Kane, J. V.; and Mollenauer, J. F.: Energy Levels of He^4 . Phys. Rev. Letters, vol. 14, no. 1, Jan. 4, 1965, pp. 15-18.
2. Zurmühle, R. W.: The $\text{D}({}^3\text{He}, \text{pn}){}^3\text{He}$, $\text{D}({}^3\text{He}, 2\text{p})\text{T}$, and ${}^3\text{He}({}^3\text{He}, 2\text{p}){}^4\text{He}$ Reactions. Nucl. Phys., vol. 72, 1965, pp. 225-235.
3. Conzett, H. E.; Shield, E.; Slobodrian, R. J.; and Yamabe, S.: Final-State Interactions in the Reaction $\text{He}^3(\text{d}, \text{t})2\text{p}$ at 24.7 and 33.4 MeV. Phys. Rev. Letters, vol. 13, no. 21, Nov. 23, 1964, pp. 625-628.
4. Jakobson, M.; Manley, J. H.; and Stokes, R. H.: The $\text{He}^3 + \text{d} \rightarrow \text{t} + 2\text{p}$ Reaction. Nucl. Phys., vol. 70, 1965, pp. 97-113.
5. Morton, B. J.; et al.: Proton-Proton Final-State Interactions in the Reactions ${}^3\text{He}(\text{d}, \text{t})2\text{p}$, $\text{d}({}^3\text{He}, \text{t})2\text{p}$, $\text{p}({}^3\text{He}, \text{d})2\text{p}$, and ${}^3\text{He}({}^3\text{He}, {}^4\text{He})2\text{p}$. Phys. Rev., vol. 169, no. 4, May 20, 1968, pp. 825-832.
6. Bilaniuk, O. M.; and Slobodrian, R. J.: Diproton and the $\text{He}^3(\text{d}, \text{t})\text{He}^2$ Reaction. Phys. Letters, vol. 7, no. 1, Oct. 15, 1963, pp. 77-79.
7. Henley, E. M.; Richards, F. C.; and Yu, D. U. L.: The Reaction $\text{d} + {}^3\text{He} \rightarrow {}^3\text{He} + \text{pp}$. Nucl. Phys., vol. A103, 1967, pp. 361-384.
8. Warner, Robert E.; and Bercaw, Robert W.: Deuteron Break-Up by 42 MeV Alpha Particles. Nucl. Phys., vol. A109, 1968, pp. 205-217.
9. Goulding, Fred S.; Landis, Donald A.; Cerny, Joseph, III; and Pehl, Richard H.: A New Particle Identifier Technique for $Z = 1$ and $Z = 2$ Particles in the Energy Range > 10 MeV. IEEE Trans. on Nucl. Sci., vol. NS-11, no. 3, 1964, pp. 388-398.
10. Blackmore, E. W.; and Warren, J. B.: Final-State Interactions in the Reactions ${}^3\text{He}({}^3\text{He}, 2\text{p}){}^4\text{He}$ and $\text{T}({}^3\text{He}, \text{np}){}^4\text{He}$. Can. J. Phys., vol. 46, no. 4, Feb. 15, 1968, pp. 233-241.
11. Chang, C. C.; et al.: Proton-Proton Final State Interaction in the ${}^3\text{He}(\text{p}, \text{pd})\text{p}$ Reaction. Phys. Letters, vol. 28B, no. 3, Nov. 25, 1968, pp. 175-177.
12. Watson, Kenneth M.: The Effect of Final State Interactions on Reaction Cross Sections. Phys. Rev., vol. 88, no. 5, Dec. 1, 1952, pp. 1163-1171.
13. Migdal, A. B.: The Theory of Nuclear Reactions with Production of Slow Particles. Soviet Phys. - JETP, vol. 1, no. 1, July 1955, pp. 2-6.
14. Schiff, L. I.: Theory of the Electromagnetic Form Factors of H^3 and He^3 . Phys. Rev., vol. 133, no. 3B, Feb. 10, 1964, pp. 802-812.

15. Preston, Melvin A.: Physics of the Nucleus. Addison-Wesley Publ. Co., 1962, p. 33.
16. Elton, L. R. B.: Introductory Nuclear Theory. Second ed., W. B. Saunders Co., 1966, p. 76.
17. Moravcsik, Michael J.: Analytic Forms of the Deuteron Wave Function. Nucl. Phys., vol. 7, 1958, pp. 113-115.
18. Perey, C. M.; and Perey, F. G.: Deuteron Optical-Model Analysis with Spin-Orbit Potential. Phys. Rev., vol. 152, no. 3, Dec. 16, 1966, pp. 923-931.
19. Collard, H.; et al.: Electron Scattering in Tritium and He³. Phys. Rev. Letters, vol. 11, no. 3, Aug. 1, 1963, pp. 132-134.
20. Rook, J. R.: The Optical Potentials for Composite Particles. Nucl. Phys., vol. 61, 1965, pp. 219-224.
21. Watanabe, Shiguo: High Energy Scattering of Deuterons by Complex Nuclei. Nucl. Phys., vol. 8, 1958, pp. 484-492.
22. Perey, F. G.; and Satchler, G. R.: The Optical Model Potential for Deuterons. Nucl. Phys., vol. A97, 1967, pp. 515-528.
23. Melkanoff, M. A.; Sawada, T.; and Cindro, N.: Optical Model Parameters for the Interaction of Intermediate Energy Deuterons with Nuclei. Phys. Letters, vol. 2, no. 2, Aug. 15, 1962, pp. 98-99.
24. Tombrello, T. A.; and Bacher, A. D.: p - p and p - n Final-State Interactions in Several Three-Body Reactions. Phys. Letters, vol. 17, no. 1, June 15, 1965, pp. 37-39.
25. Frank, R. M.; and Gammel, J. L.: Elastic Scattering of Protons by He³ and T. Phys. Rev., vol. 99, no. 5, Sept. 1, 1955, pp. 1406-1410, fig. 2.
26. Haybron, R. M.: (p - p) and (n - n) Scattering Lengths from (³He, d) and (t, d) Reactions. Nucl. Phys., vol. A112, 1968, pp. 594-602.
27. Lefevre, H. W.; Borchers, R. R.; and Poppe, C. H.: Neutrons from Deuteron Breakup on D, T, and He⁴. Phys. Rev., vol. 128, no. 3, Nov. 1, 1962, pp. 1328-1335.
28. Poppe, C. H.; Holbrow, C. H.; and Borchers, R. R.: Neutrons from D + T and D + H. Phys. Rev., vol. 129, no. 2, Jan. 15, 1963, pp. 733-739.
29. Jarmie, Nelson; Silbert, M. G.; Smith, D. B.; and Loos, J. S.: Proton-Triton Elastic Scattering Below 1 MeV. Phys. Rev., vol. 130, no. 5, June 1, 1963, pp. 1987-1989.

30. Werntz, C.; and Brennan, J. G.: Existence of H^4 and Li^4 . Phys. Letters, vol. 6, no. 1, Aug. 15, 1963, pp. 113-115.
31. Cerny, Joseph; Détraz, Claude; and Pehl, Richard H.: Li^4 and the Excited Levels of He^4 . Phys. Rev. Letters, vol. 15, no. 7, Aug. 16, 1965, pp. 300-303.

TABLE I. - OPTICAL MODEL PARAMETERS

Set	Optical model parameters				References
	Real part of optical potential, V_O , MeV	Imaginary part of potential, W_O , MeV	Trion charge radius, $r_O = 1.25 \times A^{1/3}$, fm	Normaliza- tion in fig- ure 5	
1	60.0	15.0	1.63	0.25	$E_d = 11.8$ MeV, various nuclei (ref. 19)
2	118.0	27.0	1.27	1.00	$E_d = 10.2$ MeV, Be (ref. 20)
3	123.0	40.0	1.22	1.70	$E_d = 11.8$ MeV, Mg (ref. 18, set b)
4	120.0	28.0	.95	.16	$E_d = 11.8$ MeV, Al (ref. 18, set b)
5	140.0	2.5	2.45	1.67	Ref. 7

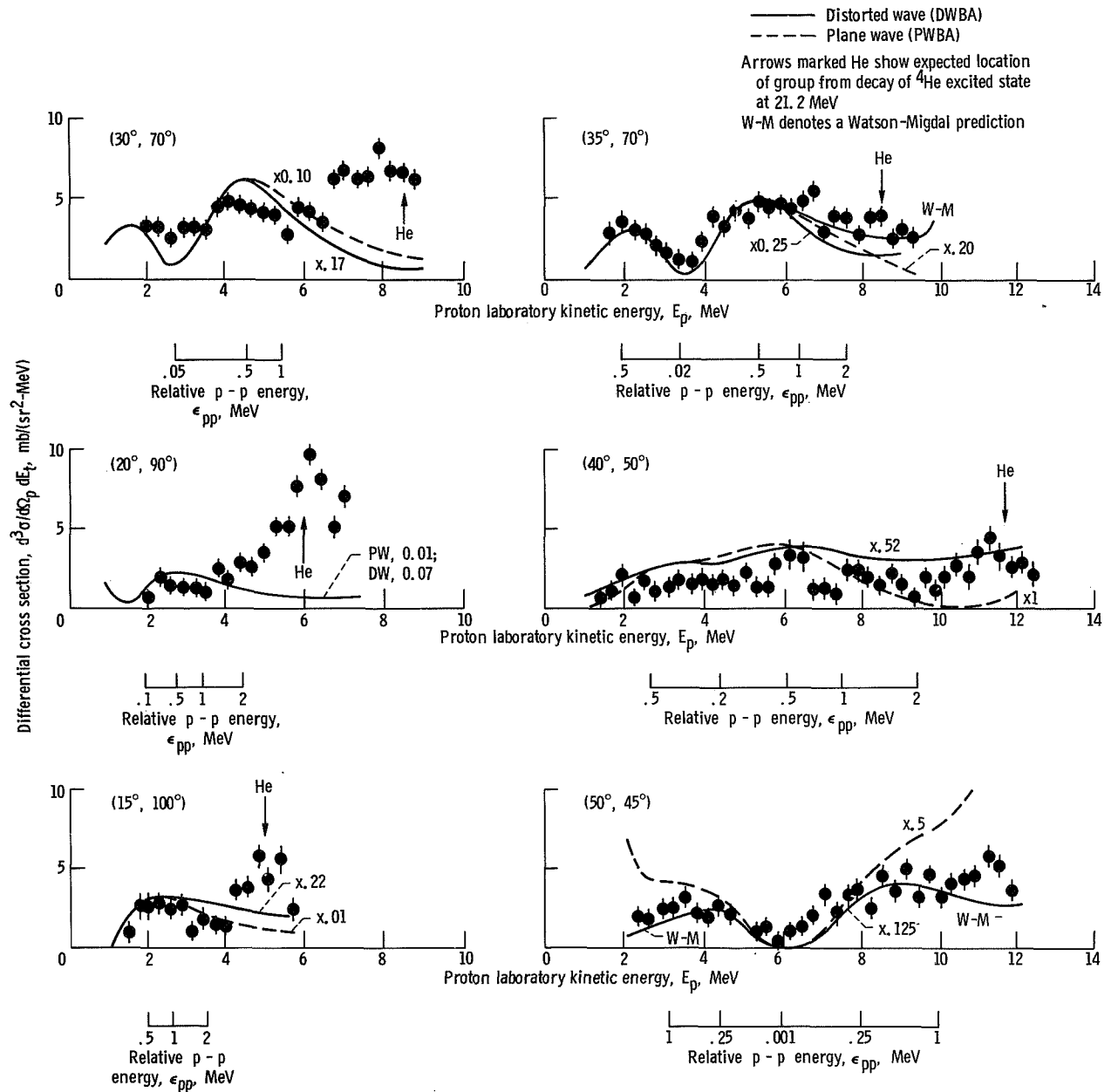


Figure 1. - Absolute differential cross sections for coincidence detection of $t + p$ from ${}^3\text{He}(d, tp)$ at 12 geometries, projected on proton energy axis. When only a solid curve is shown, the PWBA and DWBA prediction coincide except for normalization.

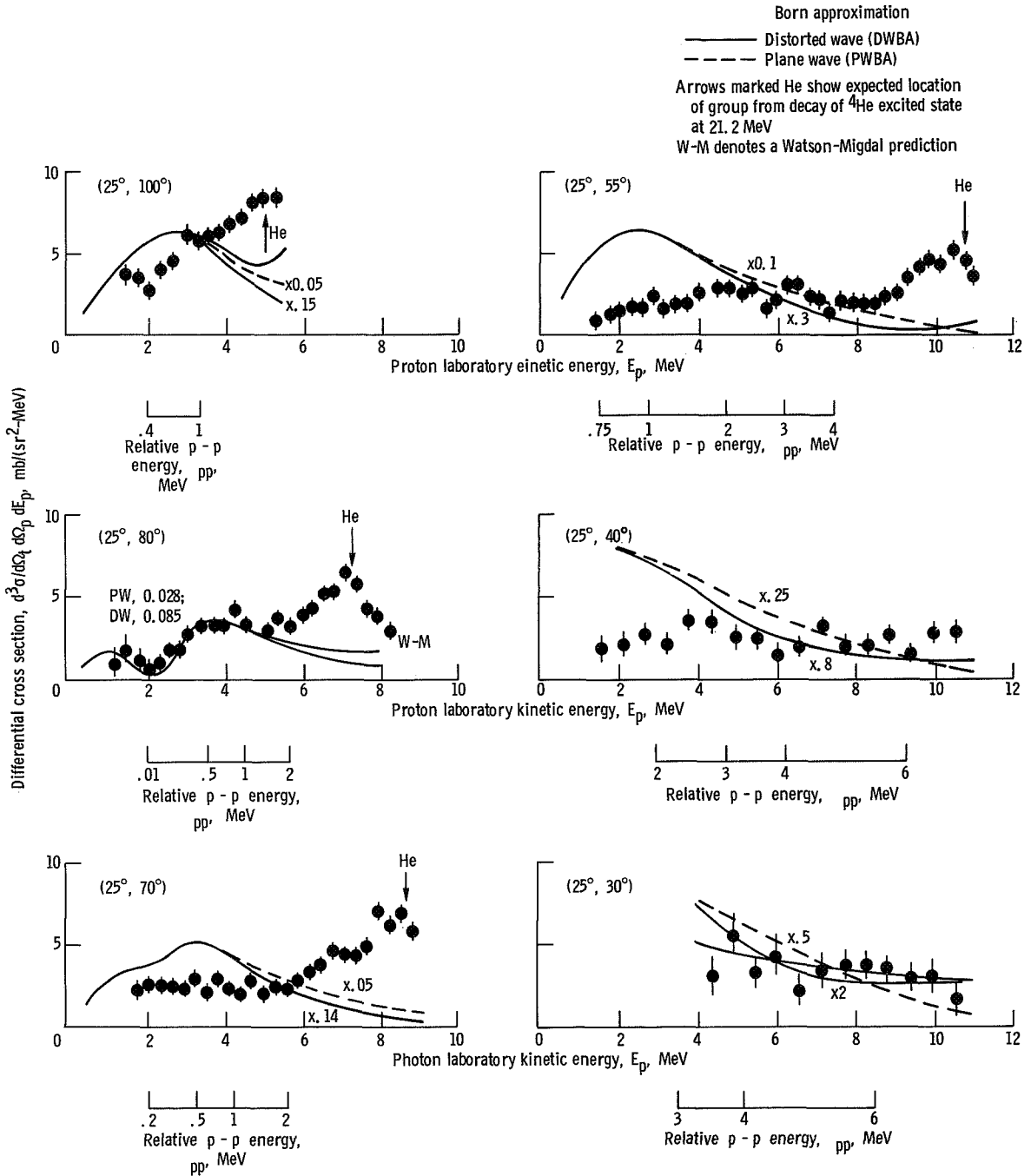


Figure 1. - Concluded.

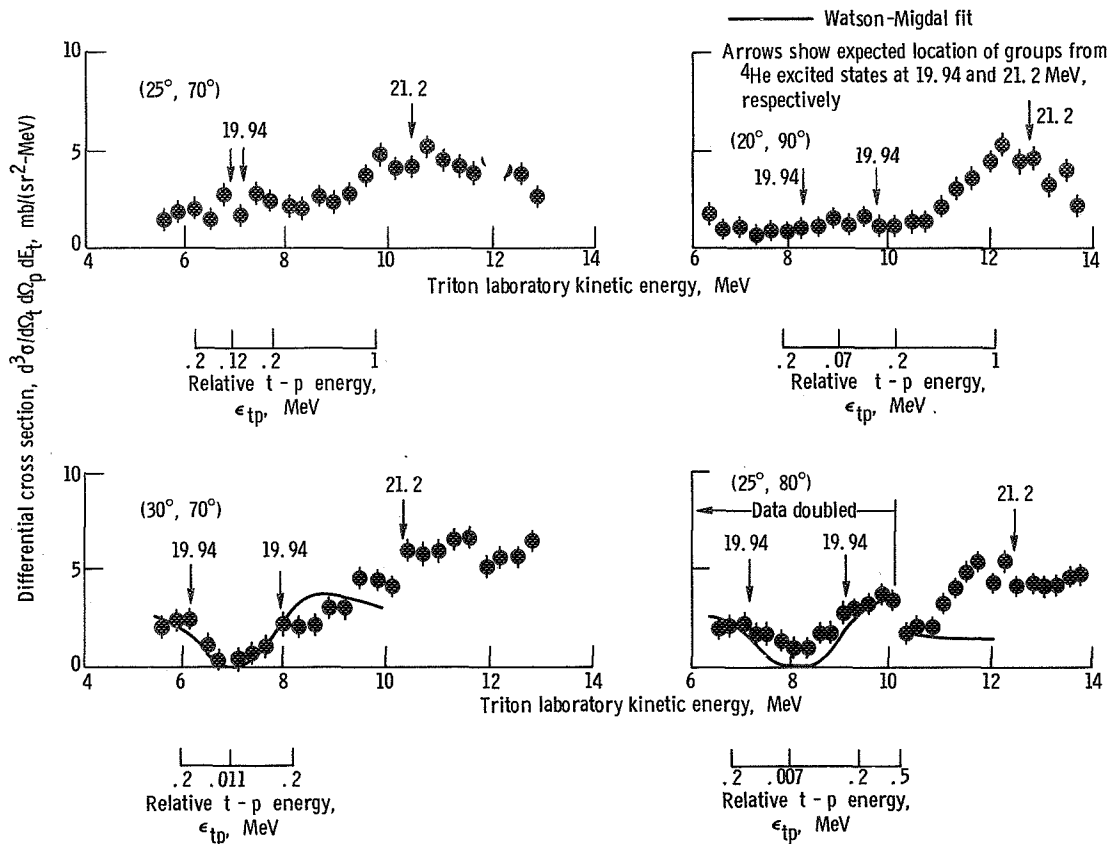
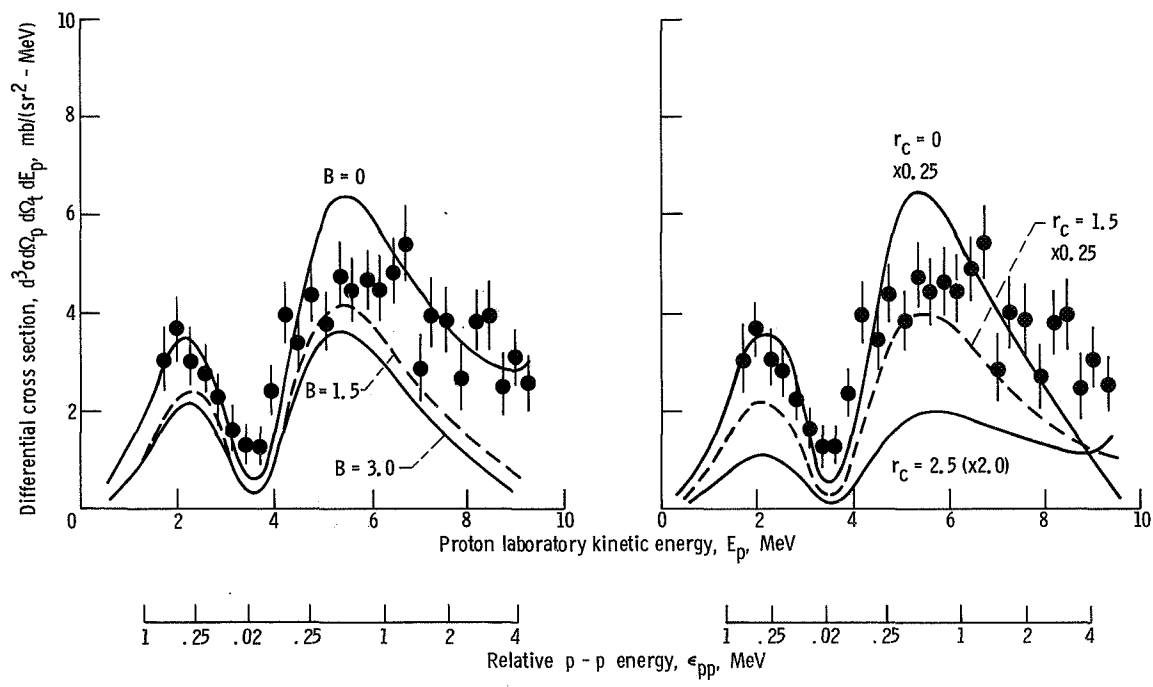


Figure 2. - Absolute differential cross sections for coincidence detection of t + p, projected on triton energy axis. Auxiliary scale give relative energy of triton plus undetected proton, in their own center-of-mass system. At (25°, 80°) data and predictions are doubled below 10 MeV to improve readability.



(a) Effect of variation of force parameter on (35°, 70°) PWBA predictions. Computed cross sections are divided by $(1 + B)^2$.
 (b) Effect of variation of cutoff radius (r_c) on (35°, 70°) PWBA predictions. Normalizing factors are shown.

Figure 3. - Effect of varying force parameter and cutoff radius on plane-wave Born approximations.

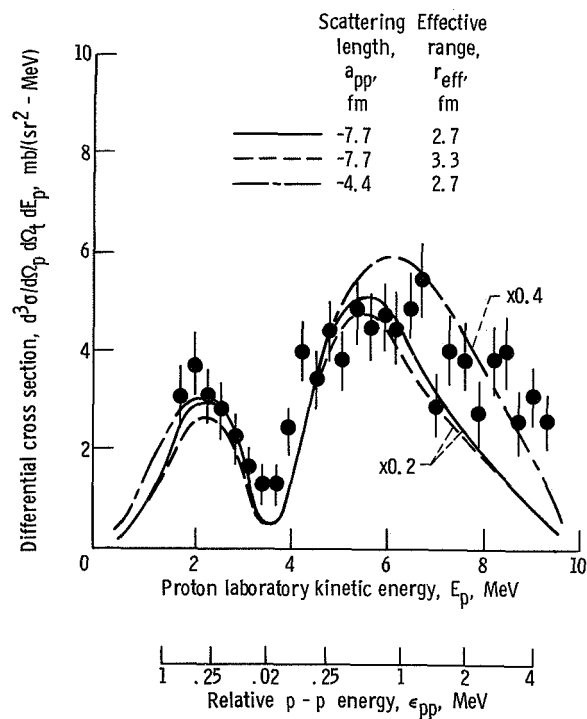


Figure 4. - Effect of variation of p - p force parameters on (35°, 70°) plane-wave Born approximation predictions. Woods-Saxon well parameters used to produce the indicated scattering lengths and effective ranges are given in text.

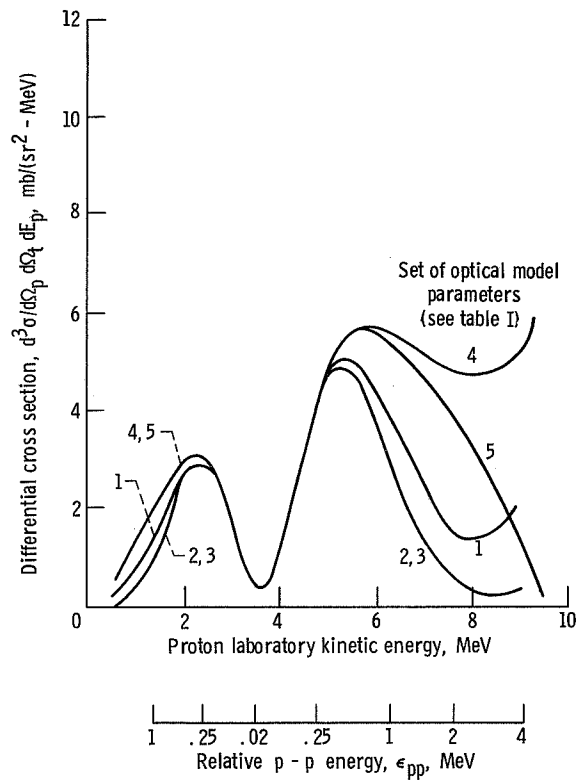


Figure 5. - Distorted-wave Born approximation predictions at $(35^\circ, 70^\circ)$ for five sets of optical model parameters listed in table I for the $d - {}^3\text{He}$ (or t - diproton) interaction.

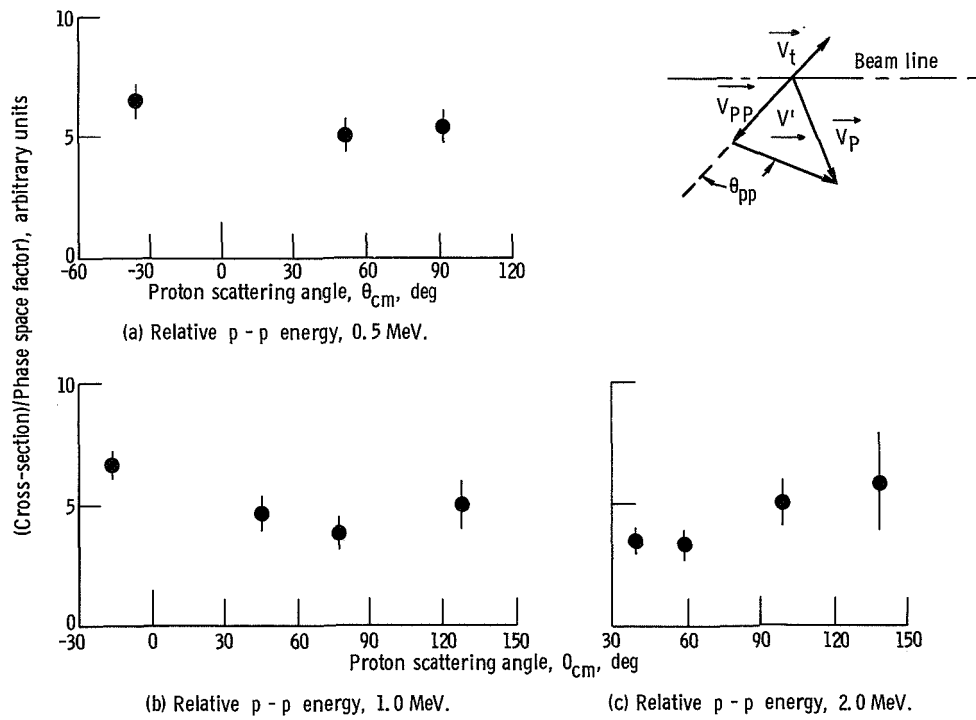
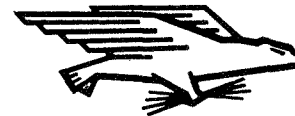


Figure 6. - Angular distributions for protons detected in coincidence with tritons at $\theta_t = 25^\circ$ in the laboratory ($55^\circ \pm 3^\circ$ in the overall center-of-mass system), for relative p - p energies of 0.5, 1.0, and 2.0 MeV. (The sketch defines the proton scattering angle θ_{pp} where V_t , V_p , and V_{pp} are the velocities of the triton, detected proton, and p - p center-of-mass, respectively, in the overall c. m. system. Thus, V' and θ_{pp} are the velocity and scattering angle of the detected proton in the p - p c. m. system.)

FIRST CLASS MAIL



POSTAGE AND FEES PAID
NATIONAL AERONAUTICS AND
SPACE ADMINISTRATION

POSTMASTER: If Undeliverable (Section 158
Postal Manual) Do Not Return

"The aeronautical and space activities of the United States shall be conducted so as to contribute . . . to the expansion of human knowledge of phenomena in the atmosphere and space. The Administration shall provide for the widest practicable and appropriate dissemination of information concerning its activities and the results thereof."

— NATIONAL AERONAUTICS AND SPACE ACT OF 1958

NASA SCIENTIFIC AND TECHNICAL PUBLICATIONS

TECHNICAL REPORTS: Scientific and technical information considered important, complete, and a lasting contribution to existing knowledge.

TECHNICAL NOTES: Information less broad in scope but nevertheless of importance as a contribution to existing knowledge.

TECHNICAL MEMORANDUMS: Information receiving limited distribution because of preliminary data, security classification, or other reasons.

CONTRACTOR REPORTS: Scientific and technical information generated under a NASA contract or grant and considered an important contribution to existing knowledge.

TECHNICAL TRANSLATIONS: Information published in a foreign language considered to merit NASA distribution in English.

SPECIAL PUBLICATIONS: Information derived from or of value to NASA activities. Publications include conference proceedings, monographs, data compilations, handbooks, sourcebooks, and special bibliographies.

TECHNOLOGY UTILIZATION PUBLICATIONS: Information on technology used by NASA that may be of particular interest in commercial and other non-aerospace applications. Publications include Tech Briefs, Technology Utilization Reports and Notes, and Technology Surveys.

Details on the availability of these publications may be obtained from:

SCIENTIFIC AND TECHNICAL INFORMATION DIVISION
NATIONAL AERONAUTICS AND SPACE ADMINISTRATION
Washington, D.C. 20546